

Searching for a resolution of BSM puzzles at accelerators and in space Mikulenko, O.

Citation

Mikulenko, O. (2024, December 12). Searching for a resolution of BSM puzzles at accelerators and in space. Retrieved from https://hdl.handle.net/1887/4172421

Version: Publisher's Version

License: License agreement concerning inclusion of doctoral thesis in the

Institutional Repository of the University of Leiden

Downloaded from: https://hdl.handle.net/1887/4172421

Note: To cite this publication please use the final published version (if applicable).

Chapter 1

Introduction

Throughout human history, physics has been an endeavor to understand complex phenomena — to find a collection of simple principles, or a model, that explains these phenomena. At the dawn of civilization, people strove to personify the natural phenomena they observe, endow the incomprehensible forces of nature with the familiar and understandable qualities of a fellow human being. It is remarkable how ubiquitous these attempts are, too: most mythologies have solar and lunar deities occupying the highest roles in the pantheon, to name the most obvious. It would not be an exaggeration to say that the pursuit of an explanation is one of our defining traits.

A crucial aspect of understanding a system is the use of empirically derived principles in order to, broadly speaking, predict the future. The essence of such a prediction is simply generalization: rearranging the parts of the internal machinery behind the given phenomenon to make complementary conclusions. If rain is an act of some anthropomorphic deity, they might be expected to share some human-like attributes. For example, they might be pleased to receive gifts in the form of sacrifices or enjoy a performance involving ritualistic dancing, and thereupon act in a desirable way. The intermediate divine explanation that possesses not only weather-related but also some independent qualities is what allows us to derive this otherwise meaningless connection.

To take it to the extreme, predicting the future is what life is about. Analyze the circumstances, identify the actions that are expected to lead to a favorable outcome, and execute them. Predicting the next solar eclipse, the existence of black holes, or predicting what happens if you arrange a set of specific components in a very specific fashion, put it into a metal box with wheels, pour some gasoline, and turn on the ignition (also referred to as the act of driving a car) — these are all predictions of what happens under certain circumstances, with varying degree of human influence on them.

The obvious advantage of making better predictions necessitates improving in

how we select better models. With the advancement of the scientific approach in the last several centuries, we have identified two main methods. The first method relies on connecting independent phenomena: finding a single root whose diverging branches can capture several seemingly unrelated things. The electric and magnetic fields were thought to be independent entities until the unified theory of electrodynamics was invented. The second method consists of finding new yet unknown phenomena that the model predicts, devising a dedicated experiment, and comparing the predictions to the actual outcome. In our example of electrodynamics, this corresponds to the prediction by James Maxwell and the following discovery by Heinrich Hertz of electromagnetic waves.

Our current understanding of the Universe is fascinatingly simple and compact, in view of how many things it explains, and based on *how* and *what*. The *how* refers to the way real-world systems universally behave and consists of two parts: relativistic quantum mechanics, which governs the behavior of particles at the smallest probed scales, and general relativity, the theory of gravity at the largest scales. Notably, the existence of these two separate parts, which are notoriously difficult to reconcile in the limit of strong gravity at microscopic scales [1, 2], indicates that some unified theory of quantum gravity is yet to be discovered.

The *what* refers to what our Universe is made of rather than how it behaves. Our most firmly established conclusion is that the Universe is a cocktail of at least 17 particles, constituting the Standard Model (SM) of particle physics as shown in Fig. 1.1, shacked vigorously to temperatures of at least several MeV or billions K to launch nuclear reactions and then let cool.

The Standard Model is a self-consistent theory that has been designed to meet the needs of our laboratory-based research. We have completed a model that does not have any substantial tension with any fully terrestrial experiment and could be an accurate description of fundamental interactions up to the quantum gravity limit. The establishment of the SM, from the neutrino prediction in the 1930s to the discovery of the Higgs boson, was a Golden Age of particle physics. New particles were predicted from the consistency of the theory, and the subsequent search for them was a win-win situation: either the prediction is correct and the theory is closer to completion, or the negative or unexpected result gives a new piece of the puzzle.

Applying this 'laboratory' particle physics to the Universe was a remarkable success [3, 4]. The theory with no relation to the cosmos had managed to predict not only the existence of micrometric electromagnetic waves, permeating the space with temperature $T=2.7\,\mathrm{K}$, but also the primordial chemical composition of the Universe. In the spirit of the scientific approach, this marks that we are on the right way towards understanding the origin and history of our Universe.

¹With the exception of experiments with reactor neutrinos.

Standard Model of Elementary Particles

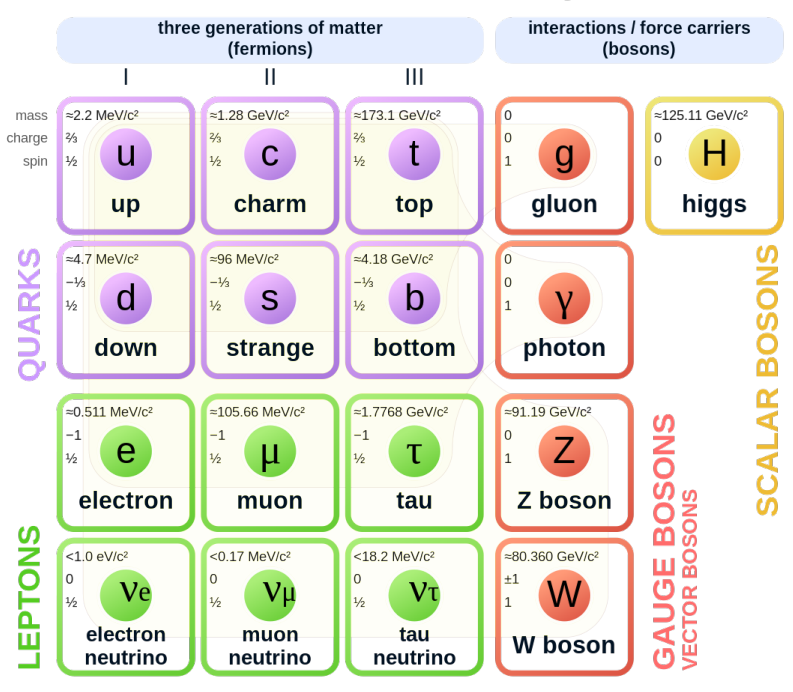


Figure 1.1: The Standard Model of particle physics: three families of fermionic quark+lepton doublets, four gauge vector bosons, and a scalar Higgs boson associated with the spontaneous symmetry breaking. *Credits: Wikipedia*.

Although cosmology and astrophysics respect the SM, they also show unequivocally that this model is far from complete. First, the Universe is filled with gravitating dark matter, which cannot be composed from particles known to us — it has to be something else. Second, the Universe prefers matter over antimatter by a tiny factor of one billionth, which, at the end of the day, is responsible for the existence of galaxies, stars, planets, and ultimately us. The origin of this factor remains a mystery, which is to be solved by new physics. Third, with the help of length scales offered by astrophysics, it was found that neutrinos, particles so light that they were thought to be massless, do have mass. The Standard Model has been constructed to account for massless neutrinos, and their masses, millions of times less than that of the electron, pose yet another challenge. Fourth, the Universe is homogeneous at the largest scales accessible to observations. However, causality, i.e. the finite speed of light, prevents the farthest observed regions from ever having any connection to each other. The properties of these patches in the sky should have been absolutely unrelated. Some new physics could drive the process of *inflation* of the Universe, expanding initially microscopic regions to extremely large sizes and making everything uniform before the known physics started to play a role.

The current situation differs drastically from the Golden Age of particle physics:

the mentioned Beyond the Standard Model (BSM) problems indicate that some ingredients are missing but provide no hints of what these pieces could be or where to search for them. This has naturally stimulated incessant attempts to envisage possible solutions to the puzzles and to guide the experimental searches. With the still-growing number of models and no actual trace of something new, the guiding for experiments gradually becomes less definitive. Many attempts have revolved around the idea that new physics should lurk at higher and higher energies. This was indeed a correct assumption for the SM, and the Large Hadron Collider (LHC) fulfilled its primary role by finding the Higgs boson [5, 6]. However, contrary to the expectations, the detectors did not shine like a Christmas tree with the signals from new hypothetical particles. The success of the energy frontier has come to a halt, and it is becoming more compelling to start looking elsewhere.

The *intensity frontier* is a possible alternative to the energy frontier that focuses on searching for feebly interacting particles (FIP). The tiny interaction strength prevents FIPs from being visible in high-energy collisions. Search for such particles requires high intensity and dedicated experimental facilities. Motivated by dark matter, many models incorporate dark or hidden sectors and FIPs play the only link between such sectors and the SM. **Intensity frontier and FIPs are the main focuses of this thesis.**

Among the many theoretical proposals, the Neutrino Minimal Standard Model ν MSM stands out by potentially solving multiple BSM problems simultaneously with a minimal adjustment of the current theory, in the spirit of the scientific approach. The model adds only three fermionic FIPs called Heavy Neutral Leptons (HNLs). The potential detectability of HNLs by the next generation experiments and their potential to answer significant cosmological and particle physics questions make them a crucial area of study.

Finally, it is necessary to mention the cosmological frontier. All BSM problems originate in space, and further exploration and study of the Universe can provide us with more insights. In this context, the study of neutrinos and their masses is the most appealing target, covered in more detail in Chapter 7. In particular, detecting the cosmic neutrino background is a straightforward goal, resembling the Golden Age search for the Higgs boson. The SM provides us with a solid prediction of the properties of relic neutrinos. The experimental detection can either confirm the prediction, which is good, or refute it, which is even better.

1.1 Problems Beyond the Standard Model

When building new reasonable theories, it is imperative to have a full picture of the BSM phenomena in mind. We list the observational evidence for these phenomena, how the SM fails to account for them, and possible solutions. Inflation is deliberately omitted from the discussion due to the lack of connection with the presented work.

Dark Matter

From the early 1930s, the term dark matter referred merely to the opposite of luminous matter. This is a gravitating mass that does not emit sufficient light to be observed in telescopes. Already in 1933, Zwicky [7] established that the amount of such invisible matter in the Coma cluster is 400 larger than that of the visible matter. The velocities of the nebulae are too high to be created by the gravitational forces of the visible matter alone.

Currently, both cosmological and astrophysical observations support the existence of dark matter as a kind of nonrelativistic matter composed of unknown particles. Alternative theories, such as modification of Newton's law [8], can explain some of the phenomena but do not show the same concordance in the large range of scales, from Mpc to Gpc, as the particle dark matter hypothesis does. Astrophysical piece of evidence is based on the local gravitational interaction at the scale of galaxies and clusters. Cosmological observations probe specifically the dynamics of ordinary matter, i.e., electrically charged electrons and nuclei, in the early Universe.

An incomplete list of astrophysical evidence consists of the rotational curves of galaxies, thermal imaging of galaxy clusters, and cluster collisions, as shown in Fig. 1.2. Spiral galaxies, like M33 [9], spin with a rotational velocity depending on the radius from the center. The outer layers farther from the bright, massive inner region should have smaller velocities as the gravitational force slowly fades away, yet the measured velocity remains constant at larger radii, indicating that the distribution of mass extends beyond the visible edges. Thermal imaging refers to the pictures of hot (keV or 10⁷ K temperature) intergalactic gas in the X-ray range [10]. The flux maps the gas density, while the temperature map imprints the gravitational potential in which gas is submerged. This combination offers an independent probe of the mass composition in galaxy clusters. The Bullet cluster [11–13] is a collision event between two galaxy clusters and has a remarkable feature. The visible gas slowed down due to the ordinary matter interaction, but most of the mass advanced unimpeded by the collision, as inferred from gravitational lensing.

Cosmological evidence is based on the two pillars of the Big Bang theory mentioned above: primordial nucleosynthesis (BBN) and cosmic microwave background (CMB). Both phenomena are sensitive to the amount of known baryonic matter. The BBN is affected because nuclear reactions begin only once the photons cool and can no longer break down the composite nuclei. The abundances of primordial elements, namely H, D, He-3, He-4, and Li-7, are a direct measure of the baryon-to-photon number density ratio $\eta_B \equiv n_B/n_\gamma \sim 6 \cdot 10^{-10}$ [20, 21], as shown in the left part of Fig. 1.3. CMB is a snapshot of the Universe at the time when charged electrons and protons bounded into neutral hydrogen, making the space transparent. In a similar fashion, the moment of CMB decoupling is affected by η_B . The most precious piece of information is stored in the tiny anisotropies ($\Delta T/T \lesssim 10^{-4}$) of the CMB



Figure 1.2: Astrophysical evidence of the existence of DM. Left: rotational velocity of stars in M33 [14]. Center: galaxy cluster Abell 1689 with an estimated gas $10^{14} M_{\odot}$ and total $10^{15} M_{\odot}$ mass [15]. Generally, galaxies contribute roughly 10% to the visible mass [16], which in turn constitutes about 15% of the total mass [17]. Credits: X-ray (blue): NASA/CXC/MIT/E.-H Peng et al; Optical (yellow): NASA/STScI. Right: Bullet cluster image, with superimposed hot gas in pink [11] and the gravitational potential in blue [12, 13], determined from weak gravitational lensing (distortion of the background picture of galaxies).

properties in the sky, discovered in 1992 [22] and measured to great precision by the recent Planck experiment [23], see the right part of Fig. 1.3. The distribution of cold and hot spots is correlated due to the complicated dynamics (e.g., sound waves) in the plasma [24]. These correlations contain an enormous amount of information about the past and current state of the Universe [19], enabling the determination of both baryonic $\Omega_b \approx 5\%$ and total matter densities $\Omega_m \approx 30\%$ separately, relative to the today's total energy density. Interestingly, the existence of nonbaryonic matter can be easily deduced from the anisotropies even without relying on an intricate procedure of decyphering the correlation spectrum. The line of reasoning is simple: the radiation pressure counteracts the gravitational collapse of charged particles. Therefore, the density inhomogeneities of baryons before CMB decoupling were at the level of the temperature fluctuations 10^{-4} ; from this value, galaxies would not have time to collapse until today [25]. Something not affected by photons should have started collapsing earlier and created potential wells for the lagging baryons.

The formation of structures provides additional constraints. First, if dark matter is fermionic, there is a lower bound on particle mass $\sim 0.5-1\,\mathrm{keV}$, known as the Tremaine-Gunn bound [26, 27]. Fermionic gas cannot go beyond the natural limit of a fully degenerate state; if DM is too light, it would not be possible to have heavy but compact objects, such as dwarf spherical galaxies. Second, DM particles cannot be too relativistic, or hot, throughout the expansion of the Universe; otherwise, they would smear inhomogeneities of the size of their free-streaming length. Therefore, a viable DM should be at least warm, with the corresponding smearing below the detection limit of, for example, Lyman- α probes [28, 29], or straight up cold with vanishing free-streaming length. For thermally produced relics (with typical momentum today similar to the CMB temperature), this translates into a lower mass limit of roughly

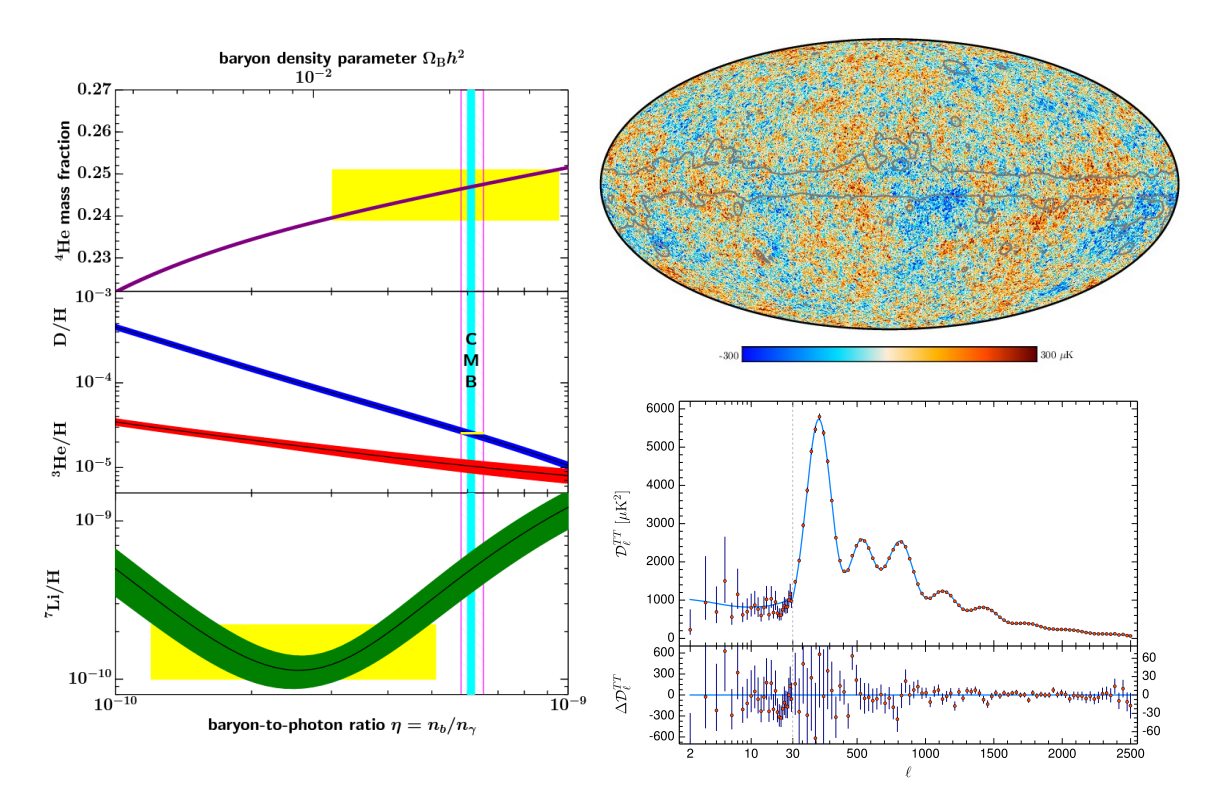


Figure 1.3: Left: SM BBN predictions (lines) and combined measurements (yellow rectangles) of primordial abundances for relevant isotopes [18] as functions of baryon-to-photon ratio η_B . The Planck measurement of η_B [19] is labeled CMB. Right: temperature map of the Universe from Planck [19] (top). Tiny temperature fluctuations $\delta T/T \lesssim 10^{-4}$ at different spots are correlated as a result of dynamics in baryon-photon plasma. These correlations (bottom) depend on the angular separation $l = 2\pi/\theta$. The position of the main peak corresponds to the distance sound waves traversed before CMB decoupling.

1 keV as well.

The combined data dictate the basic properties of dark matter particles: they are sufficiently nonrelativistic (and, obviously, massive), cosmologically stable, and interact feebly with the SM and itself (which includes being electrically neutral). The list of requirements still leaves an impressive amount of possible candidates with masses spanning orders of magnitudes; see Fig. 1.4.

A few general considerations are useful in the context of DM models. Particles that decouple from the early plasma while being relativistic have number density $n_{\rm DM}$ similar to that of photons n_{γ} , contributing to the energy density today at the level of

$$\Omega_{\rm DM} \sim 80 \cdot \left(\frac{n_{\rm DM}}{n_{\gamma}}\right) \cdot \left(\frac{m_{\rm DM}}{1 \, {\rm keV}}\right)$$

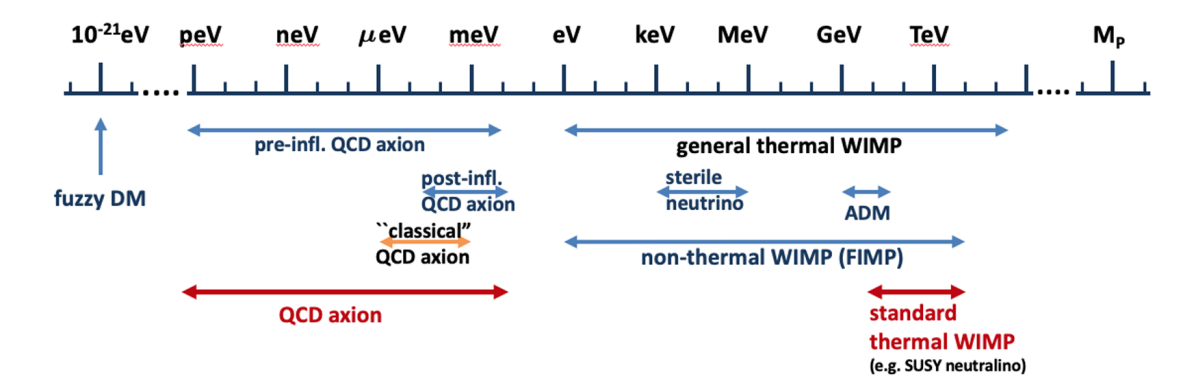


Figure 1.4: The mass range of possible DM candidates from [30]. Above Planck mass M_p , there also exists an option of primordial black holes [31].

which overcloses the Universe for masses above the bound dictated by free-streaming. The possible ways to avoid the problem are as follows:

1. Weekly Interacting Massive Particles (WIMPs) - heavy (above GeV) particles with a sufficiently high annihilation rate that ensures that they decouple while being nonrelativistic and the relic abundance is suppressed. With a weak-like cross-section, the resulting energy density is [32]

$$\Omega_{\rm DM} \sim 0.05 - 0.10 \, \frac{(10 \, {\rm TeV})^{-2}}{\langle \sigma v \rangle_{\rm freeze-out}}$$

naturally close to the observed value. The picobarn scale of the cross-section stimulated the active search for direct DM-nucleus/electron scattering; see [30] for the list of existing and proposed experiments.

- 2. Feebly/super-weakly interacting particles particles that never reach thermal equilibrium [33]. Their number density slowly builds from the interactions of the SM plasma [34] or through decays of WIMPs [35]. Alternatively, long-lived heavy particles can dilute DM density through a delayed reheating of the SM plasma [36].
- 3. Ultra-light axion dark matter [37, 38]. Thermal production of ultra-light particles would lead to extremely insufficient number density. Instead, such particles are expected to be produced via the *misalignment* mechanism. At very early stages, the classical axion field has flat potential and acquires some arbitrary initial value ϕ_0 . During the expansion, the potential develops a minimum at some other point $\phi_m \neq \phi_0$, forcing the field to start oscillating around the minimum and behaving as dark matter.

Baryon asymmetry of the Universe

The Universe today does not contain antimatter, except for particles that are created in cosmic rays. In the Big Bang model, the earliest stage we have experimental evidence of corresponds to the temperature of about 1 MeV, when neutrinos decoupled and determined the outcome of BBN. Just a little earlier, the temperature of the plasma could reach 150 MeV, sufficient to melt protons and neutrons into quark-gluon plasma [39, 40]. At this point, the number densities of light u, d quarks become comparable to that of photons $n_q \sim n_{\bar{q}} \sim n_{\gamma}$. The situation has a remarkable implication: the initial state should have an asymmetry between quarks and antiquarks at the level of η_B , i.e., contain an extra quark per every billion quark-antiquark pairs. To postulate such a small number, neither strictly zero nor of order one, as the initial condition is unnatural. A more appealing explanation is that the asymmetry is generated dynamically from a symmetric state, in the process of baryogenesis. Reviews on the topic are given in, e.g., [41, 42].

Any process that can generate baryon asymmetry must satisfy a set of three *Sakharov conditions* [43]. The conditions and their status within the Standard Model are as follows.

1. Violation of the baryon number.

The most straightforward requirement is to have any process that can change the number of baryons. Such processes do exist in the SM and are called the sphaleron transitions (Fig. 1.5): thermal jumps between topologically nonequivalent vacuum configurations of the $SU_L(2)$ fields [44, 45]. Charge conservation is violated by gauge fields through Adler-Bell-Jackiw anomaly [46–49]; in a sphaleron transition, three left (anti)quarks and a (anti)left lepton emerge from the Dirac sea, leaving B-L the only conserving number. Sphaleron transition rate is faster than the expansion of the Universe in the temperature range $100 \,\text{GeV} \lesssim T \lesssim 10^{12} \,\text{GeV}$.

2. C and CP violation.

If the model is invariant under relabeling particles and antiparticles (what C stands for), symmetry considerations guarantee that no $B \neq 0$ can be generated. C and parity P symmetries are known to be violated by weak interactions. However, without additionally broken CP, the violation would simply correspond to a disbalance between left particles/antiparticles and an exactly opposite disbalance in the right-handed sector. For a true particle/antiparticle asymmetry, CP must be violated as well.

In the Standard Model, CP violation is present and manifests itself in oscillations of neutral mesons, e.g., $K^0 - \bar{K}^0$ [51]. On the Lagrangian level, CP transforms all numerical parameters into their complex conjugate; therefore,

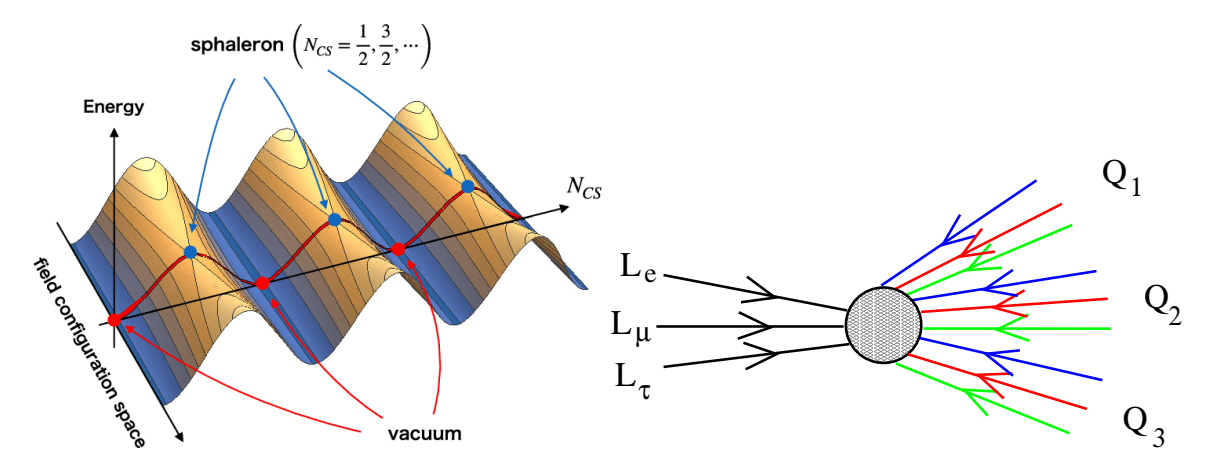


Figure 1.5: Left: an illustration of infinitely dimensional space of gauge fields [50]. There are infinitely many pure gauge configurations with zero energy, separated into classes that differ by their topological properties, i.e. cannot be continuously transformed into each other. The sphaleron is a saddle point, corresponding to the minimal energy that separates two vacuum manifolds. Right: a sphaleron transition [42] — once the field jumps out of one vacuum into another, it redefines the Dirac sea, which we observe as an appearance of quarks and leptons.

a violation happens only in the presence of some *physical*, i.e., not affected by field redefinitions, complex phase in the model. Such a phase is present in the CKM matrix: in fact, it can only appear in (at least) a 3×3 unitary matrix, which led to the prediction of the third quark generation by Kobayashi and Maskawa [52].

Physically, CP violation can parametrized as the relative difference in the rates

$$\delta = \frac{\Gamma(X \to Y) - \Gamma(\bar{X} \to \bar{Y})}{\Gamma(X \to Y) + \Gamma(\bar{X} \to \bar{Y})}$$

Worth noting, the rate difference is not visible at tree-level diagrams (since $|M_{\text{tree}}|^2 = |M_{\text{tree}}^*|^2$) and appears only once the loop corrections are taken into account. The CKM-induced asymmetry can be conveniently parameterized with the Jarlskog invariant [53] and happens to be extremely suppressed [54–56]:

$$\delta \sim \frac{m_t^4 m_b^4 m_c^2 m_s^2}{m_W^{12}} J \sim 10^{-20}$$

ten orders of magnitude below the observed baryon asymmetry to begin with. The SM does not contain a sufficient amount of CP violation.

3. Departure from thermal equilibrium.

If baryon number violating processes are very rapid, quarks and antiquarks tend to reach the same equilibrium Fermi-Dirac distribution regardless of the initial

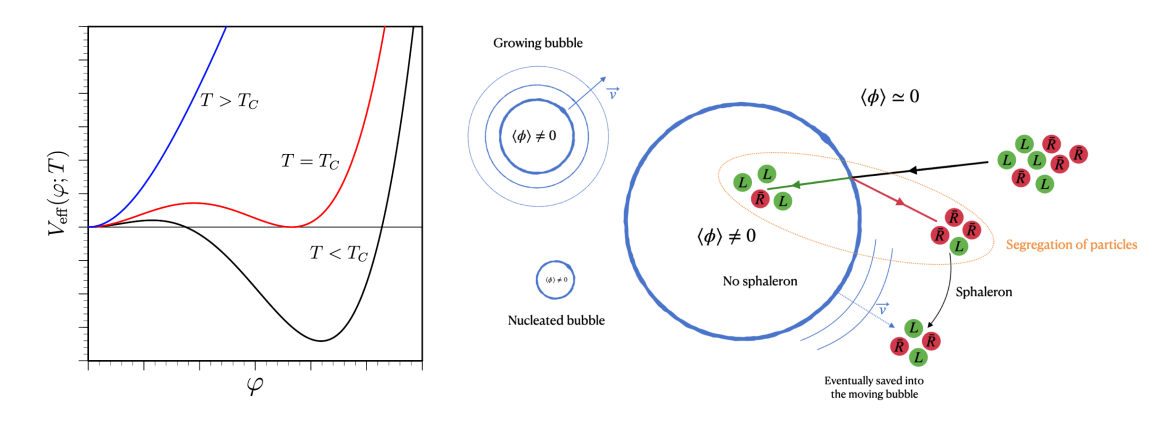


Figure 1.6: Left: free energy for first-order phase transition as a function of the classical field value ϕ for different temperatures [59]. The energy minimum jumps into the broken phase as temperature decreases below $T < T_C$. Right: creation of a bubble with broken phase that expands and generates the baryon asymmetry during its motion through the plasma [60].

state. An excess of baryons is rapidly converted into antibaryons by B-violating processes, which then convert antibaryons back, at a different but still rapid rate. This exchange relaxes the difference between particles and antiparticles to zero. Thermal equilibrium washes out the asymmetry; therefore, the asymmetry must be generated after the departure of equilibrium.

In the Standard Model, a high sphaleron rate out of equilibrium may be possible in the violent process of first-order phase transition. At high temperatures, the electroweak symmetry is not broken, and the vacuum value of the Higgs field is zero $\langle \phi \rangle = 0$. Once the temperature decreases, the thermal potential develops another minimum that corresponds to the broken phase. The Higgs field tries to jump into the second minimum through nucleation: the thermal creation of bubbles with the broken phase that expand and ultimately fill the space. A passage of the bubble wall through the plasma is a nonequilibrium process that can lead to a residual baryon asymmetry. The described picture, shown in Fig. 1.6, would be perfect, except for one thing: the conditions required for the first-order phase transition are not fulfilled in the SM. Specifically, the mass of the Higgs boson $M_H=125\,\mathrm{GeV}$ is too high for a successful phase transition, only possible below $M_{H,\mathrm{crit.}}\lesssim 90\,\mathrm{GeV}$ [57, 58]. Without any new physics, the transition is a smooth crossover between the vacua which does not introduce any deviations from equilibrium.

In summary, the SM provides all the necessary ingredients for baryogenesis but fails to account for the observed baryon asymmetry. Several mechanisms have been suggested that can resolve the puzzle and produce sufficient asymmetry.

GUT baryogenesis. Grand Unification Theories [61–63] are a class of models

that combine the SM gauge symmetry $SU(3) \times SU(2) \times U(1)$ into a single simple group. Quarks and leptons are combined into representation multiplets of the full group. Therefore, there should be some gauge bosons that transform q into l. Since such bosons have not been found, they are expected to be heavy; moreover, they are typically associated with the scale of $10^{16} \,\text{GeV}$ [64], where the running couplings of the three SM interactions seem to converge to a single value. These new bosons would also induce proton decay with the lifetime $\tau \sim M_X^4/m_p^5 \sim 10^{32} \,\text{years} \,(M_X/10^{16} \,\text{GeV})^4$, where m_p is the proton mass and M_X is the mass of the new bosons. Existing constraints $\tau(p \to e^+\pi^0) > 10^{34} \,\text{years}$ [65] disfavor GUT scenarios, although do not exclude.

Electroweak baryogenesis. This class refers to models that address the weak points of SM baryogenesis, specifically the Higgs sector. A richer scalar sector can accommodate additional CP-violating parameters and modify the thermal potential to achieve a first-order phase transition. Examples of such extensions include the scalar portal (see below), the two-Higgs doublet model, and the Minimal Supersymmetric Model, see [66] and references therein. The new scalar particles can be searched directly at collider experiments. Moreover, these models predict intense emission of gravitational waves (GW) from bubble collisions, which can be potentially probed by future GW experiments [67].

Leptogenesis. Fukugita and Yanagida [68] suggested that the asymmetry generation can be confined to the lepton sector; the B-L conserving sphaleron processes convert produced L into B afterward. In the SM, nonzero B-L number is redistributed by sphalerons in thermal equilibrium as [69]:

$$B = \frac{28}{79}(B - L), \qquad L = -\frac{51}{79}(B - L) \tag{1.1.1}$$

Lepton number violation appears naturally if the SM is extended with Majorana fermions N. The Yukawa interaction with Higgs and leptons for several new species can incorporate CP-violation, depicted diagrammatically in Fig. 1.7. In the standard thermal leptogenesis, the requirement that N have sufficient CP-violation and abundance after going out of equilibrium fixes the mass scale of the new fermions above $10^9 \, \text{GeV}$. The qualitative analysis of the generated asymmetry in a toy model of thermal leptogenesis can be found in [70], together with a list of other possible scenarios.

Affleck-Dine mechanism. This mechanism [71, 72] differs considerably from other mechanisms in its use of a classical scalar field. It is best illustrated with a toy model:

$$\mathcal{L} = |\partial \phi|^2 - m^2 |\phi|^2 - \lambda |\phi|^4 + \epsilon (\phi^4 + \phi^{*4}) + [\phi O + \text{h.c.}]$$

where $m, \lambda > 0$ are real parameters, ϕ is a complex scalar field, and O is a gauge invariant effective operator with $B - L \neq 0$: a simplest example is $O \sim [\epsilon^{ijk} d_{R,i} u_{R,j} u_{R,k} e_R]$

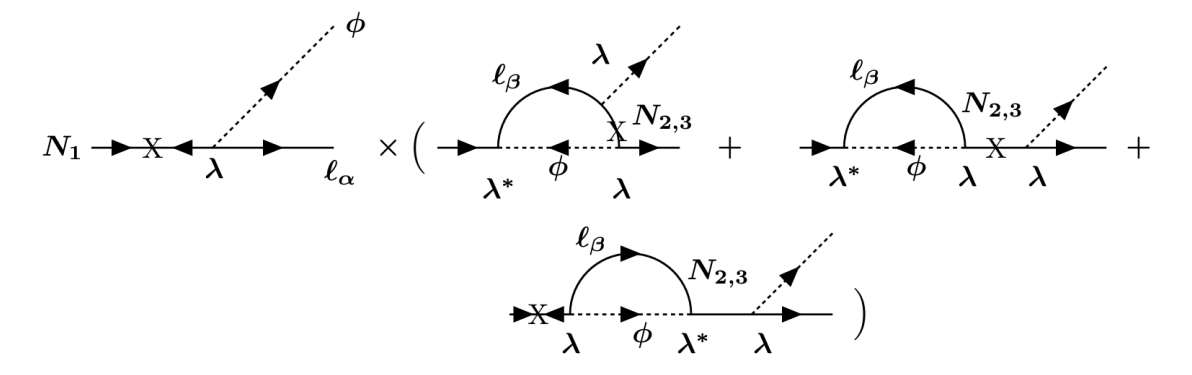


Figure 1.7: The schematic depiction of CP-violation in the decay of Majorana fermion N_1 from [70]. The loop diagrams include contributions from heavier N.

with i, j, k being the SU(3) color indices.

For $\epsilon = 0$, the model has both CP-invariance $\phi \to \phi^*$, $O \to O^*$ and a symmetry which can be associated with B-L charge: $\phi \to e^{i\alpha}\phi$, $O \to e^{-i\alpha}O$. Nonzero complex ϵ violates both symmetries. Classical dynamics of ϕ drives oscillations of the B-L charge $n_B \sim \int (\dot{\phi}^*\phi - \dot{\phi}\phi^*) d^3x$, which freezes out at some point due to the expansion of the Universe. After that, n_B is transformed into quarks and leptons due to the decay of ϕ .

Neutrino masses

Neutrinos were proposed by Pauli [73] to explain varying electron energy in β -decays and were subsequently discovered in the inverse β -decay [74]. The electron energy spectrum had no indication that this new particle has nonzero mass, and so the neutrino was believed to be massless.

In 1957, Pontecorvo suggested that neutrinos, being neutral, can exhibit oscillations between flavors [75, 76], similarly to the recently discovered $K^0 - \bar{K}^0$ oscillations. The states produced in weak interactions ν_{α} can be superpositions of particles that evolve in time independently:

$$|\nu_{\alpha}\rangle = U_{\alpha i}|\nu_{i}\rangle, \quad \langle\nu_{\beta}|e^{-i\hat{H}_{\text{free}}t}|\nu_{\alpha}\rangle = \sum_{i} U_{\beta i}^{*}e^{-iH_{i}t}U_{\alpha i}$$

where ν_i are states that diagonalize the free Hamiltonian with the corresponding H_i eigenvalues. To rephrase, neutrinos oscillate if they have different masses (thus are massive) and the mass eigenstates do not coincide with the interacting states — the unitary U, called Pontecorvo-Maki-Nakagawa-Sakata matrix [77], is not unit.

Forty years later and seventy years after Pauli's original proposal, oscillations of neutrinos were confirmed [78, 79], solving at the same time the long-standing solar neutrino deficit problem [80]. The oscillation data [81] only provides the values of PMNS matrix angles and two squared mass differences $\Delta m_{ij}^2 = |m_i^2 - m_j^2|$. The

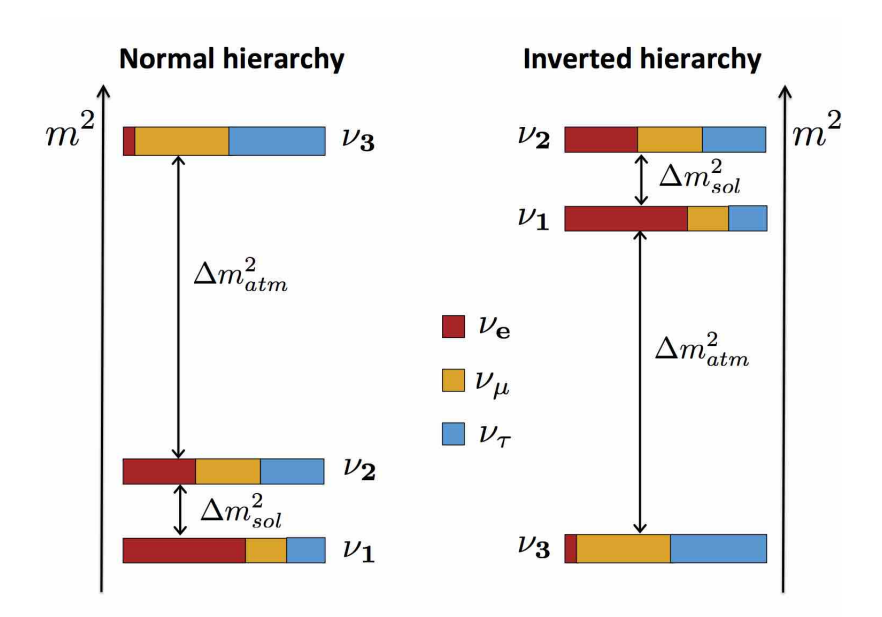


Figure 1.8: Two possible options for the neutrino mass ordering: ν_1 and ν_2 are separated by the smaller splitting $\Delta m_{\rm sol.}^2$, while the third species ν_3 can be heavier or lighter than the pair. Credits: [84]

latter is related to the fact that all observed neutrinos are ultrarelativistic. Hence the oscillation phase is $|H_i - H_j|t = 2\Delta m_{ij}^2 l_{\nu}/E_{\nu}$ for a given neutrino energy E_{ν} and traveled distance l_{ν} . The smaller neutrino mass splitting is provided by the measurements of solar neutrinos $\Delta m_{\rm sol}^2 \sim (9\,{\rm meV})^2$, with subtlety in the form of matter-induced Mikheev-Smirnov-Wolfenstein effect [82, 83]. The larger mass splitting $\Delta m_{\rm atm}^2 \sim (50\,{\rm meV})^2$ comes from the analysis of atmospheric neutrino flux composition as a function of zenith angle [78], which controls the oscillation length l_{ν} . Notably, neither the mass of the lightest species nor the ordering, or hierarchy, of neutrino masses is known. Two possible neutrino hierarchies, called normal and inverse, are shown in Fig. 1.8. The mass splittings provide the minimal limit on the overall scale of neutrino masses, $\sum m_{\nu} \gtrsim 60\,{\rm meV}$ (NH), $100\,{\rm meV}$ (IH). On the other hand, the upper limit is severely constrained by cosmology and β -decay experiments down to $\sum m_{\nu} \lesssim 0.2-1\,{\rm eV}$, leaving only a narrow range of possible values. For further details, see Chapter 7.

In Weinberg's model of leptons [85], which is the electroweak part of the SM, gauge interactions are chiral and the fundamental fields are left and right fermions, glued together through the Higgs vacuum expectation value. The experimental facts that some fermions have masses and both right and left components are charged dictate the model structure. Neither of these two statements could be applied to neutrinos. A potential right-handed species ν_R has to be neutral under all gauge interactions and is essentially Russell's teapot of the model.

Nevertheless, neutrinos do have masses and require some modification to the

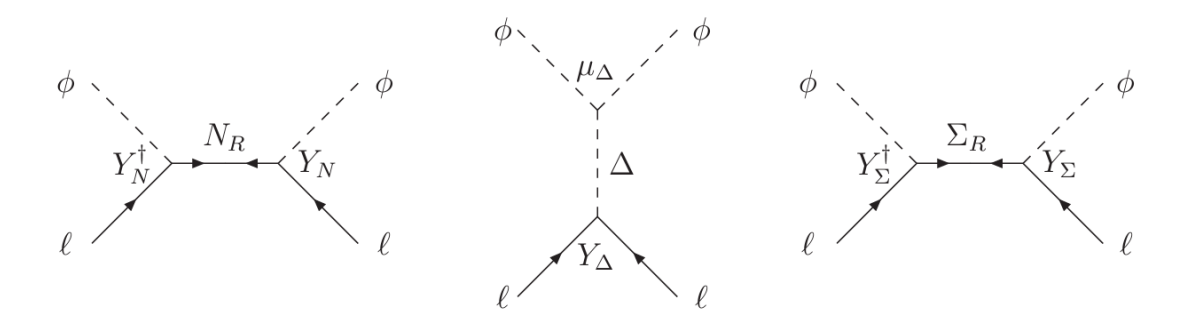


Figure 1.9: Tree realizations of the Weinberg operator: type-I (singlet fermion N), type-II (triplet scalar Δ), and type-III (triplet fermions Σ) seesaw mechanism. *Credits:* [88]

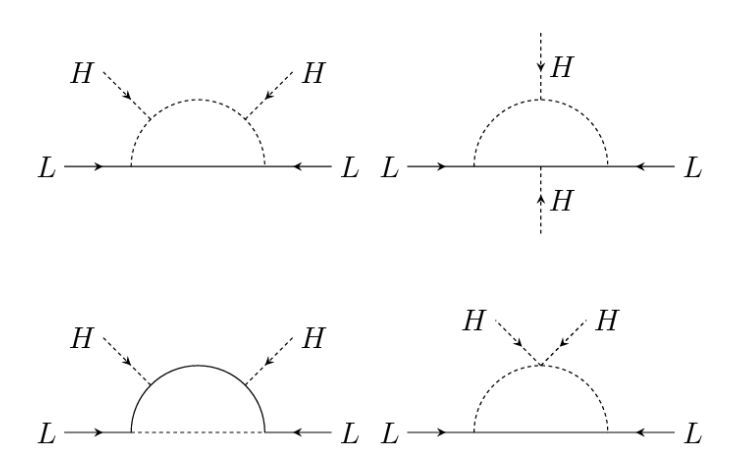


Figure 1.10: Loop diagrams that generate neutrino masses [89].

SM. To complicate things, the mass can be introduced in various ways. Unlike other fermions, neutrinos are neutral and can have Majorana mass, generated via the dimension-5 Weinberg operator [86] after spontaneous symmetry breaking:

$$\mathcal{L} \supset \frac{L^c L \tilde{H} \tilde{H}}{\Lambda} \Longrightarrow m_{\nu} \bar{\nu}^c \nu, \qquad m_{\nu} \sim \frac{v^2}{\Lambda}$$

with $L=(l,\nu)$ being the left lepton doublet and $\tilde{H}=i\sigma_2H$ is the conjugated Higgs doublet. New physics that defines the scale Λ is responsible for generating naturally small neutrino masses, $m_{\nu} \ll v \ll \Lambda$. There are exactly three ways to generate the Weinberg operator at the tree level [87], collectively called the seesaw models or seesaw mechanism. These three realizations are shown in Fig. 1.9. Another natural way to explain the small neutrino mass is via loop-induced suppression, see Fig. 1.10. In this case, the number of possibilities is somewhat larger, closer to thousand [89] for 1-loop diagrams only. Neutrinos can also be Dirac fermions, with their own right-handed counterparts. The questions remain: What are the properties of these new degrees of freedom, how to test them, and why is the neutrino mass so small? The answers

would definitely involve more new particles; for example, a small mass can originate from the loop diagrams [90], similar to the Majorana case.

1.2 Heavy neutral leptons and ν MSM

The Neutrino Minimal Standard Model (ν MSM) [91, 92] is arguably the minimal extension of the Standard Model, in terms of new degrees of freedom, that can deal with all the mentioned BSM problems. The model introduces three Heavy Neutral Leptons (HNLs): one keV-scale dark matter candidate N_1 and two N_2 , N_3 with masses at or above the GeV scale. The Lagrangian is:

$$\mathcal{L} = \mathcal{L}_{SM} + i\bar{N}_I \partial N_I - \left[\frac{M_I}{2} \bar{N}_I^c N_I - F_{\alpha I} (\bar{L}_{\alpha} \tilde{H}) N_I + \text{h.c.} \right]$$

where I = 1, 2, 3, $L_{\alpha} = (l, \nu)_{\alpha}$ being the left lepton doublet, $\alpha = e, \mu \tau$, $\tilde{H} = i\sigma_2 H$ is the conjugated Higgs doublet, M_I are Majorana masses of the HNLs, and $F_{\alpha I}$ are Yukawa couplings.

HNLs are parameterized by their corresponding masses m_I and mixing angles $U_{\alpha I} \equiv |\theta_{\alpha I}|$, where $\theta_{\alpha I} \equiv F_{\alpha I} v/m_N$. The first N_1 species serves as a dark matter candidate, while the two heavier N_2 , N_3 are responsible for neutrino masses and leptogenesis. Below, we summarize their properties.

keV-scale dark matter N_1

The sterile neutrino N_1 serves as a warm dark matter candidate [93, 94]. The viable mass window for such a particle lies in a quite narrow range around keV, determined by the Tremaine-Gunn bound from below and the effective stability of the DM particles together with constraints from the X-ray emission from DM-dominated objects [95] from above.

The DM candidate N_1 is produced in interactions of active neutrinos in the early plasma [34]. The crucial role here plays the Mikheev-Smirnov-Wolfenstein effect, which suppresses the $\nu \to N_1$ conversion rate at high energies and prevents sterile neutrinos from thermalizing too early. Instead, the abundance of DM with the thermal spectrum slowly builds up, with the peak production rate around the $T \sim 150\,\mathrm{MeV}$ temperature, to the level of:

$$\Omega_N h^2 \sim 0.1 \left(\frac{U_{L,\text{DM}}^2}{10^{-7}}\right) \left(\frac{m_N}{1 \text{ keV}}\right)^2$$

Moreover, large lepton asymmetry in the early plasma, if present (see, e.g., [96–99] for the possible sources), might create the resonance condition for the $\nu-N_1$ mixing, resulting in an additional contribution to the DM abundance with a markedly

nonthermal and colder spectrum [98–102], compatible with structure formation constraints [28, 103–105].

X-ray observations provide strong constraints on the width of the radiative $N_1 \to \nu \gamma$ decay [105, 106]. The limits on the corresponding mixing angle imply a negligible seesaw contribution of N_1 to neutrino masses (< 0.1 meV). Given the very strong dependence of the lifetime on the mass, $\tau \sim m_N^{-5}$, the parameter space above 50 keV requires extremely feeble interaction strength in conflict with the production mechanisms to account for the observed DM abundance. The recent measurement of the primordial ⁴He abundance [107] does tend to favor nonzero lepton asymmetry $\xi_e = 0.05^{+0.03}_{-0.02}$.

Additional, more sophisticated mechanisms, such as nonminimal coupling to gravity, may contribute to the DM abundance [108–110] as well.

GeV-scale HNLs N_2 , N_3

HNLs produce neutrino masses via the type-I seesaw mechanism [111–118]. After the spontaneous symmetry breaking, Dirac mass term appears in the Lagrangian:

$$\mathcal{L} \supset m_D \nu_\alpha N_i - \frac{M_I}{2} \bar{N}_I^c N_I, \qquad m_D \equiv \frac{F_{\alpha I} v}{\sqrt{2}}$$

and after diagonalization leads to neutrino mass of the order $m_{\nu} \sim m_D^2/M_I$. Two known neutrino mass splittings are compatible with two massive neutrino states, corresponding to the minimal amount of two right-handed neutrinos N_2 , N_3 . Moreover, the neutrino oscillation data allow us to partially reconstruct the properties of the mixing matrix $\theta_{\alpha I}$ (reduced to 3×2 by dropping N_1), using the Casas-Ibarra parameterization [119]:

$$\theta = iU^{\text{PMNS}} \left(m_{\nu}^{\text{diag}} \right)^{1/2} R \left(M_N^{\text{diag}} \right)^{-1/2} , \qquad (1.2.1)$$

where U^{PMNS} is the PMNS matrix, m_{ν}^{diag} , M_N^{diag} are the diagonalized mass matrices of neutrinos and HNLs (3×3 and 2×2 correspondingly), and R is a complex 3×2 matrix that satisfy $RR^T = \text{diag}(0,1,1)$ for normal and diag(0,1,1) for inverse neutrino mass hierarchy. The parametrization has two major implications. First, the absolute values of R can be made arbitrarily large, meaning that the mixing angles are not restricted to the seesaw level $U_{\text{seesaw}}^2 \sim m_{\nu}/m_N$ but can be, in principle, much larger. Second, this approximate symmetry limit of $U \gg U_{\text{seesaw}}$ requires the mixing angles of the HNL pair to converge $U_{\alpha 2} \approx U_{\alpha 3}$, drastically reducing the possible parameter space.

GeV-scale HNLs can account for baryon asymmetry through the mechanism of resonant leptogenesis [120–123]. The difference from thermal leptogenesis lies in the enhancement of CP-violation from oscillations between HNLs if they are mass-degenerate. The CP violation from Fig. 1.7 can be large once the mass splitting

between the decaying and the intermediate HNL is of the order of their decay width $|M_2 - M_3| \sim \Gamma_{2,3}$. This effect extends the parameter space of the HNLs for successful leptogenesis below the electroweak scale down to the mass of a few GeV, see numerous studies [102, 124–140].

The prospect of collider searches for HNLs has been extensively studied; see [141, 142] for reviews. An incomplete list of studies includes analyses of SHiP [143], DUNE [144, 145], LHC-based experiments [146–150, VIII], and future colliders [151–154, IX]. In addition to this, HNLs can be constrained by astrophysics and cosmology. This includes HNL effects on the BBN [155–157], CMB [158, 159], and supernova explosions [160–162], as well as searches in cosmic rays [163–165]. Finally, indirect searches such as electroweak precision measurements [166–168] and charge lepton number violation [169–171] also provide constraints on HNLs.

Further remarks

The ν MSM is a complete model that, in principle, provides all the predictions in itself as a function of the properties of the three new fermions. In particular, it should predict the amount of DM from the first principles, accounting for the accumulation of lepton asymmetry at lower temperatures that enhances DM production. The relation between the fundamental parameters of the model and the predictions is, however, extremely non-trivial. HNLs are only coupled to the left-handed SM particles, which induces a chiral imbalance that triggers the generation of persistent large-scale magnetic fields below the electroweak scale [172, 173]. The fully coupled system exhibits complex behavior, with the backreaction of magnetic fields on the baryon and (resonant) DM production, and is still to be understood. It is still unknown whether the magnetic fields from this dynamics can survive in the primordial plasma for a sufficiently long time and be related to the large-scale magnetic fields observed in intergalactic space [174–177].

The final remark concerns inflation. The three new fermions cannot be responsible for inflation, and some other mechanism is needed. Notably, no new degree of freedom is required: ν MSM can incorporate inflation through a non-minimal interaction between the Higgs field and gravity [178, 179]. With this adjustment, ν MSM solves all the BSM problems without a need for new particles above the electroweak scale and can be a valid description of fundamental interaction up to the Planck scale.

1.3 The thesis

The thesis consists of the following chapters.

Chapter 2 presents a uniform approach for the analysis of the sensitivity to various Feebly Interacting Particles for the presented experimental proposals. A dedicated experiment is required for searching for FIPs, and SHiP in the current geometry provides the optimal sensitivity.

Chapter 3 summarizes constraints on heavy neutral leptons in the ν MSM. Direct searches use simplified and unrealistic scenarios of HNL coupling to a single lepton flavor. The presented analysis combines the two-HNL seesaw model with the bounds imposed by direct searches, BBN, and leptogenesis.

Chapter 4 discusses the prospects of new experiments, with a focus on SHiP, to identify the properties of a potentially discovered FIP signal and establish the connection between the new particle and the BSM problems. Depending on the particle mass, tens of observed events may suffice to differentiate between the portal models. In the context of ν MSM, we define the sensitivity required to reject the two-HNL seesaw model for a generic HNL.

Chapter 5 is dedicated to the analysis of HNL searches at a future high-energy muon collider, which can explore feebly interacting particles above the electroweak scale, with masses up to a few TeV. The potential sensitivity of an experiment at a muon collider can reach the parameter space of successful leptogenesis with 3 degenerate HNLs. Moreover, it is possible to differentiate between the Majorana and Dirac cases for a new HNL and scrutinize the signal even further to test the degeneracy hypothesis.

Chapter 6 analyzes the phenomenology of a degenerate HNL pair in the Left-Right Symmetric Model (LRSM). The LRSM restores the symmetry between left and right particles by extending the gauge symmetry with a right-handed $SU_R(2)$ group, spontaneously broken at a scale much heavier than the electroweak one. Neutrino masses are generated by both type-I and type-II seesaw mechanisms, thus affecting the relation between the HNL couplings to different lepton flavors. Right-handed interactions modify HNL phenomenology, opening up the possibility of searching for a light DM candidate in the decay of heavy HNL.

Chapter 7 delves into another aspect of neutrino physics: detection of relic neutrino background. Neutrino masses are tightly related to cosmology. The proposed PTOLEMY experiment can detect relic neutrinos via a β neutrino capture, which results in an electron with energy slightly exceeding, by two neutrino masses, the maximally allowed energy in the β -decay. Reconstruction of the electron energy with such extreme resolution is limited by the many-body effects, emerging from the interactions of the target isotopes with the substrate they are attached to. The chapter analyzes the applicability of heavy isotopes, less affected by many-body physics, as potential targets for relic neutrino capture experiments.